Evaluating the spike in the symptomatic proportion of SARS-CoV-2 in China in 2022 with variolation effects: a modeling analysis

Salihu S. Musa [a, b, c], Shi Zhao [d], Ismail Abdulrashid [e], Sania Qureshi [f, g], Andrés Colubri [a, **], Daihai He [b, *]

[a] Department of Genomics and Computational Biology, University of Massachusetts Chan Medical School, Worcester, MA, 01605, USA
[b] Department of Applied Mathematics, Hong Kong Polytechnic University, Hong Kong SAR, China
[c] Department of Mathematics, Aliko Dangote University of Science and Technology, Kano, Nigeria
[d] School of Public Health, Tianjin Medical University, Tianjin, 300070, China
[e] School of Finance and Operations Management, The University of Tulsa, 800 South Tucker Dr., Tulsa, OK, 74104, USA
[f] Department of Basic Sciences and Related Studies, Mehran University of Engineering and Tech., Jamshoro, Pakistan
[g] Department of Computer Science and Mathematics, Lebanese American University, Beirut, Lebanon

ARTICLE INFO

ABSTRACT

Despite most COVID-19 infections being asymptomatic, mainland China had a high increase in symptomatic cases at the end of 2022. In this study, we examine China's sudden COVID-19 symptomatic surge using a conceptual SIR-based model. Our model considers the epidemiological characteristics of SARS-CoV-2, particularly variolation, from non-pharmaceutical intervention (facial masking and social distance), demography, and disease mortality in mainland China. The increase in symptomatic proportions in China may be attributable to (1) higher sensitivity and vulnerability during winter and (2) enhanced viral inhalation due to spikes in SARS-CoV-2 infections (high transmissibility). These two reasons could explain China's high symptomatic proportion of COVID-19 in December 2022. Our study, therefore, can serve as a decision-support tool to enhance SARS-CoV-2 prevention and control efforts. Thus, we highlight that facemask-induced variolation could potentially reduces transmissibility rather than severity in infected individuals. However, further investigation is required to understand the variolation effect on disease severity.

1. Introduction

As the world continued to return to normalcy from the impacts of the COVID-19 pandemic, China has witnessed a heightened rate of COVID-19 cases in December 2022 (China CDC Weekly; World Health Organization), with devastatingly

* Corresponding author. Department of Applied Mathematics, Hong Kong Polytechnic University, Hong Kong Special Administrative Region of China.
** Corresponding author. Department of Genomics and Computational Biology, University of Massachusetts, Medical School, MA, 01605, USA.
E-mail addresses: Andres.Colubri@umassmed.edu (A. Colubri), daihai.he@polyu.edu.hk (D. He).

high transmissibility and severity, which was seemingly the highest since the start of the epidemic in Wuhan in late December 2019.

It has been postulated that the severity of COVID-19 may be proportionate to the viral inoculum that initiates the infection in human host (Cai, Bowe, Xie, & Al-Aly, 2021; Gandhi & Rutherford, 2020a). Biologically, an inoculum differs from a vaccine. A vaccine is a suspension administered to stimulate body's immune system by promoting the production of antibodies (Guallar et al., 2020). At the same time, inoculum refers to introducing biological material such as cells, viruses, or immune serums into the body to incite immune response and allow the growth and reproduction of microorganisms (Biology Online; Guallar et al., 2020; Van Damme, Dahake, Van de Pas, Vanham, & Assefa, 2021). Thus, it is imperative to investigate whether non-pharmaceutical intervention (NPI) control policies (such as universal facial masking) help in reducing the SARS-CoV-2 viral inoculum, which could result in less severe COVID-19—a hypothesis referred to as the "variolation hypothesis" (Cai et al., 2021; Gandhi & Rutherford, 2020a). Variolation was initially used for the smallpox virus - a process where people susceptible to smallpox are inoculated with material taken from a vesicle of a person with smallpox with the intent of causing milder infection and subsequent immunity (Gandhi & Rutherford, 2020a; Koelle et al., 2022); however, it was never purposeful for SARS-CoV-2. According to Gandhi and Rutherford (Gandhi & Rutherford, 2020a), SARS-CoV-2 variolation is a as transmission by tiny inocula that penetrates facemasks.

Previous reports suggested that facemasks do nothing more than minimize SARS-CoV-2 transmission (Gandhi & Rutherford, 2020b; Koelle et al., 2022); they are primarily used to reduce transmission intensity rather than as a proxy for vaccination or mitigate the severity of COVID-19. A study by Gandhi & Rutherford (Gandhi & Rutherford, 2020a) highlighted that universal masking may be considered a form of "variolation" for COVID-19 and could generate immunity, thereby slowing disease transmission and severity. This hypothesis has received substantial criticism due to its unjustified conclusion and lack of proper evidence/data (Brosseau, Roy, & Osterholm, 2020; Rasmussen, Escandón, & Popescu, 2020). The authors have responded positively in (Gandhi & Rutherford, 2020b) and emphasized the need for further investigation to determine the effects of facemask-induced variolation for COVID-19 transmission (Bielecki et al., 2021; Gandhi & Rutherford, 2020a; Levine & Earn, 2022). Subsequently, Trunfio et al. (Trunfio et al., 2021) also investigated the effect of the facemask-induced variolation hypothesis; they found that there was likely no link between the viral load of index cases and the severity of COVID-19 secondary cases. A more recent study by Koelle et al. (Koelle et al., 2022) also emphasized that facial masks do no more than prevent infection. Moreover, universal facial masking has been one of the pillars of COVID-19 pandemic control—it helped reduce the transmissibility of the disease (Abaluck et al., 2022; Aydin et al., 2020; Gurbaxani, Hill, Paul, Prasad, & Slayton, 2022; Howard et al., 2021) and ensured the reduction of a significant proportion of new cases (Gandhi, Beyrer, & Goosby, 2020c; Gandhi and Rutherford, 2020a, 2020b). Although face masks do not entirely prevent the transmission of respiratory infections, masked individuals are likely to inhale fewer infectious particles (Levine & Earn, 2022; Van Damme et al., 2021).

Epidemiological modeling plays a key role in shedding light and understanding on the dynamics and control of infectious diseases. Mathematical models enable researchers to simulate and predict disease spread, assess interventions' impact, and guide public health decision-making by quantifying the intricate interactions between viruses, hosts, and the environment. Epidemiologists can use these models to better explain how diseases spread, estimate essential epidemiological parameters, and analyze intervention scenarios to devise more efficient disease prevention, control, and mitigation processes.

The objective of the present work is to mathematically investigate a sudden increase in symptomatic proportions of SAR-CoV-2 cases in mainland China, which occurred toward the end of 2022 and raised concerns about why symptomatic proportion was so high despite suggestions from several previous studies indicating that most COVID infections were asymptomatic (Abaluck et al., 2022; Aydin et al., 2020; Guallar et al., 2020; Levine & Earn, 2022; Louie et al., 2022; Nogrady, 2020; Del Rio & Malani, 2022; Eikenberry et al., 2020; Ferguson et al., 2020). Through qualitative modeling analysis, we assess potential factors driving the symptomatic proportion of SARS-CoV-2 in China towards the end of 2022 and provide more insight into the intervention measures. Our study also aims to provides comprehensive analysis on factors influencing symptomatic proportions of SAR-CoV-2 in China, offering valuable insights for public health policy and practice, as well as preparedness plans.

2. Methods

This section briefly explains the conceptual model formalism for assessing the seemingly high symptomatic proportion of SARS-CoV-2 in mainland China towards the end of 2022.

2.1. A conceptual model

The model designed in this study describes the epidemiological dynamics of COVID-19 transmission in mainland China using a conventional SIR-based model framework (Anderson & May 1991; Kermack & McKendrick, 1927) to investigate the sudden increase in symptomatic proportions of COVID-19 cases in China. The model considers two forms of infection: the usual infection and the facemask-induced variolation infection. Our model is an extension of the model proposed in (Levine & Earn, 2022) with the incorporation of asymptomatically and symptomatically infection transmission paths to investigate the sudden increase in the number of COVID-19 cases in China, as well as to assess the potential facemask-induced variolation effects. Specifically, we adopted the classical Susceptible-Exposed-Infectious-Removed (SEIR) dynamic model by

incorporating asymptomatically and symptomatically infection transmission paths, which is more appropriate in modeling COVID-19 dynamics and plays a crucial role in understanding the general transmission of the disease (Lin et al., 2020; Ngonghala et al., 2020; Tang et al., 2020). This is particularly crucial since using a more suitable model leads to more accurate estimates of key epidemiological parameters, such as reproduction numbers, exponential growth rate, and serial interval, which in turn lead to more accurate predictions of disease burden, which helps in preparedness plans against future epidemics or pandemics.

We assume that all individuals are identical and that the population is uniformly mixed. Therefore, we do not differentiate between scenarios where low-quality facemasks are worn by individuals and scenarios where only a portion of the population wears higher-quality masks. Consequently, we presume that masks are distributed randomly to individuals. Infected individuals with milder symptoms can move to varioladed-infected class (indicating that facemask-induced variation plausibly reduce disease severity). However, if the infected individuals have severe symptoms, they move to symptomatically infected individuals (who may then progress to seriously severe disease and may die), indicating that facemask-induced variation might not have effect on disease severity. Others are individuals with no symptoms, also known as silent transmitters, who can recover or die naturally. Notably, effect of variation was captured through a proportion of infections with milder symptoms $(1 - v)$, i.e., facemask-induced variation. Note also that milder infections are likely less transmissible; however, the effective infectious period for severe disease is less than that of milder infections since severely infected individuals are less likely to move around (maybe isolated); in other words, they have a lower contact rate. Consequently, three distinct scenarios were considered—milder diseases, lower transmission rates, and potentially shorter infectious periods—all contributing to the overall infections. We account for the likelihood of immunity decline but assume that it lasts the same time following moderate or severe infections (Levine & Earn, 2022).

Following (Levine & Earn, 2022; Musa et al., 2020), we split the total human population at time t, represented by $N(t)$, into sub-populations of individuals susceptible to SARS-CoV-2 infection, $S(t)$; asymptomatically infected individuals, $I_a(t)$; symptomatically infected individuals (those with severe symptoms), $I_1(t)$; $I_a(t)$; symptomatically severe infectious individuals (critically ill), $I_2(t)$; individuals who die due to COVID-19, $D(t)$; individuals recovered from the usual infection, $R(t)$; individuals infected due to variation (or facemask-induced varioladed infection), $I_v(t)$; and individuals who recovered from varioladed infection, $R_v(t)$; so that

$$N(t) = S(t) + I_a(t) + I_1(t) + I_2(t) + I_v(t) + R(t) + R_v(t).$$

The proposed model is depicted in Fig. 1; the state variables and model parameters (Table 1) fulfill the following system of non-linear ordinary differential equations (ODEs):

$$
\begin{aligned}
\frac{dS}{dt} &= \pi - \zeta S + \theta(R + R_v) - \mu S, \\
\frac{dI_a}{dt} &= \eta v \zeta S - (\tau_a + \mu) I_a, \\
\frac{dI_1}{dt} &= (1 - \eta) v \zeta S - (\tau_1 + \mu) I_1, \\
\frac{dI_2}{dt} &= (1 - \varphi) \tau_1 I_1 - (\tau_2 + \delta + \mu) I_2, \\
\frac{dI_v}{dt} &= (1 - v) \zeta S - (\tau_v + \mu) I_v, \\
\frac{dR}{dt} &= \tau_a I_a + \varphi \tau_1 I_1 + \tau_2 I_2 - (\theta + \mu) R, \\
\frac{dR_v}{dt} &= \tau_v I_v - (\theta + \mu) R_v, \\
\frac{dD}{dt} &= \delta I_2.
\end{aligned}
\tag{1}
$$

From model (1), the force of infection is formulated as follows:

$$\zeta = \sum_{i=1}^{i=4} \zeta_i = \frac{\beta(I_a + \kappa_1 I_1 + \kappa_2 I_2) + \beta_v I_v}{N}, \tag{2}$$

where $\frac{\beta(I_a + \kappa_1 I_1 + \kappa_2 I_2)}{N}$ and $\frac{\beta_v I_v}{N}$ represent transmission due to usual infection and infection due to variation (facemask-induced varioladed infection). We also assumed that $\kappa_2 < \kappa_1 < 1$, implying that I_a is likely to transmit higher than I_1, and I_1 is more likely to transmit higher than I_2. This is because critically ill people are less likely to move around. We set the state variable $D(t)$ to measure the number of COVID-19-deceased individuals to keep track of COVID-19-related deaths (for calibration and quantification of model parameters).
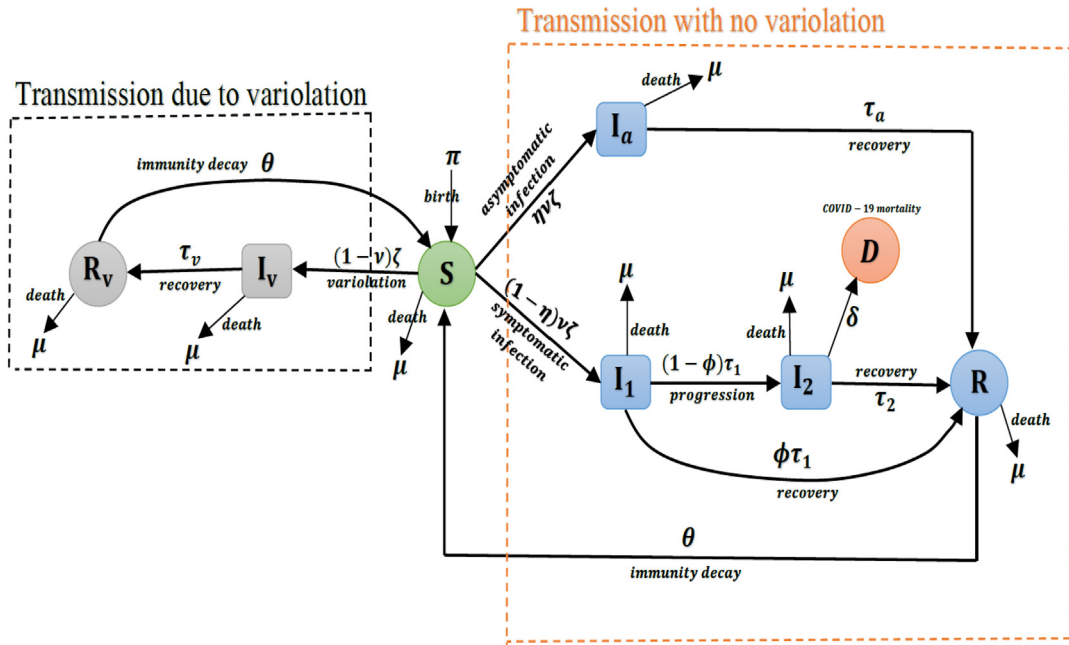
Fig. 1. A diagrammatical representation of the model (1). Solid arrows designate transitions, and expressions after arrows show the per *ca-pita* flow rate between compartments. The compartments inside the orange box represent the usual COVID-19 transmission (i.e., transmission with no variolation), while the compartments inside the black box represent infection due to variolation.

Table 1
Epidemiological description of the state variables and parameters of model (1).

Variable	Description
S	Susceptible
I_a	asymptomatically infectious
I_1	Symptomatically (severe) infectious
I_2	Symptomatically (critically ill) infectious
I_v	Variolated (mild) infectious
R, R_v	Recovered
Parameter	
π	Birth rate
μ	Natural death rate
β	Transmission rate due to usual infection
β_v	Transmission rate due to variolation
υ	Probability of infection per contact
η	Proportion of infection without clinical symptoms
ϕ	Proportion of infectious individuals that will not generate severe COVID-19
$\tau_j (j = a, 1, 2, v)$	recovery rates
θ	Immunity decay rate
δ	disease-induced death rate
κ_1, κ_2	Modification parameter for the decrease of infectiousness

2.2. Basic reproduction number

Here, we computed the basic reproduction number ($\mathcal{R}_0$) of the model (1) by adopting the next-generation matrix (NGM) technique as described in (Van den Driessche & Watmough, 2002). The $\mathcal{R}_0$ represents the number of secondary cases that a typical primary case would cause during the infectious period in a wholly susceptible population (Diekmann, Heesterbeek, & Metz, 1990; Musa et al., 2020; Van den Driessche, 2017; Van den Driessche & Watmough, 2002).

Through direct calculation of the NGM, we obtained $\mathcal{R}_0$ as follows:.

$$\mathcal{R}_0 = \rho(FV^{-1}) = \mathcal{R}_a + \mathcal{R}_1 + \mathcal{R}_2 + \mathcal{R}_v, \tag{3}$$

where

$$\mathcal{R}_a = \frac{\beta \eta \upsilon}{p_1}, \quad \mathcal{R}_1 = \frac{\beta(1-\eta)\upsilon\kappa_1}{p_2}, \quad \mathcal{R}_2 = \frac{\beta(1-\eta)\upsilon(1-\varphi)\kappa_2\tau_1}{p_2 p_3}, \quad \text{and} \quad \mathcal{R}_v = \frac{\beta_v(1-\upsilon)}{p_4},$$

where $p_1 = \tau_a + \mu$, $p_2 = \tau_1 + \mu$, $p_3 = \tau_2 + \delta + \mu$, and $p_4 = \tau_v + \mu$.

Therefore, $\mathcal{R}_0$ can be further interpreted by breaking down into three components as follows: new infections contributed by contacts with asymptomatically infected, symptomatically infected (mild and severe), and facemask-induced (variolated) infected individuals, respectively, i.e., $\mathcal{R}_a$, $\mathcal{R}_i = \mathcal{R}_1 + \mathcal{R}_2$ and $\mathcal{R}_v$. See Appendices A1-A3 for more details on the $\mathcal{R}_0$ computation and other analytical results obtained.

It is imperative to note that the reproductive number $\mathcal{R}_0(t)$, which is the focus here, should not be confused with the effective reproductive number $R_e(t) = R_0(t)*S(t)$ used in other contexts (Jewell & Lewnard, 2022; Levine & Earn, 2022; Lin et al., 2020), which we purposefully omitted in this paper. This is because we intend to evaluate the impact of mitigation measures such as lockdowns, which directly impact R_0 (through the contact/transmission rate).

2.3. Data fitting and model parameters

To validate the model, we employed Pearson's chi-square distribution and the least squares method (Hussaini, Okuneye, & Gumel, 2017; Ngonghala et al., 2020) and fitted the model to the COVID-19 situations reported (daily and cumulative) in China for the period of 1−31 December 2022. The model was randomly simulated 5000 times, and reasonable fitting results were obtained. The data were obtained from the public domain of the WHO dashboard for COVID-19 situation reports (World Health Organization) (see Appendix A4 for details). R Statistical software version 4.1.1 was used for the simulations and validation processes. Fig. 2 depicts the fitting results using reasonable model parameters. Key parameters were estimated from the fitting process; see Table 2 and Appendix A4. The outcome of the model fittings suggests that the model could be used to predict and analyze the dynamics of SARS-CoV-2 in a community.

We did not include variolation data from our model analysis and simulation processes due to its unavailability at the time of the study. However, we intend to extend our analysis with variolation data once it becomes publicly accessible. Thus, experimental variolation datasets will be integrated into the model to estimate crucial epidemic metrics (such as reproduction number, exponential growth rate, generation time, etc.) and evaluate the potential effects of variolation or facemask-induced variolation on the spread of COVID-19. In the meantime, the model was validated using COVID-19 available data from
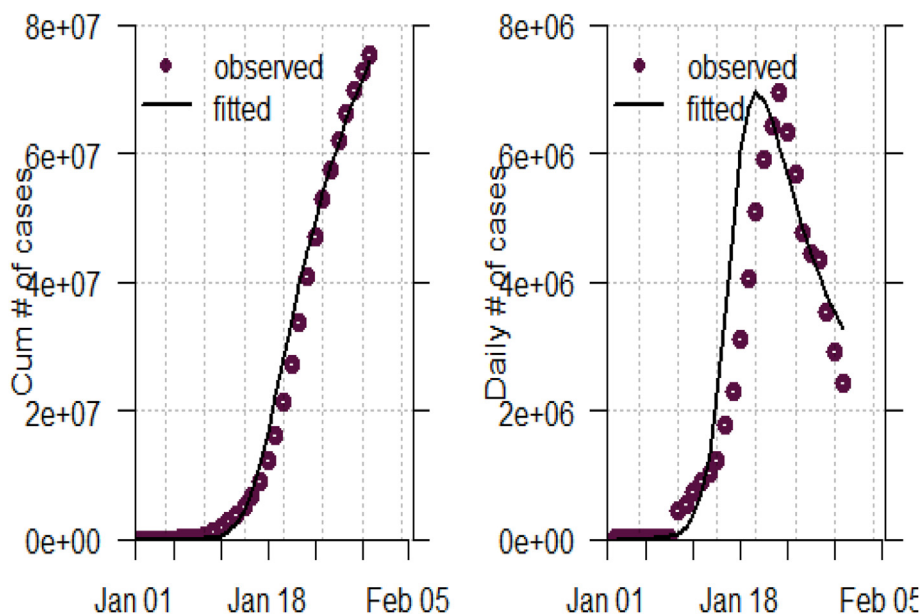
Fig. 2. Model fitting results using China's COVID-19 datasets for 2022 The dark brown color in each panel reflects the observed COVID-19 cases, while the black curves represent the model prediction based on the reported data. The left panel and right panel are the fitting results using the cumulative and daily number of COVID-19 cases, respectively. Parameter values used are given in Table 2.

Table 2
Summary table for parameters values of model (1).

Parameter	default value (range)	units	sources
π	6.77 per 1000	per day	(Statista)
μ	3.544×10^{-5}	per day	(The World Bank)
β	0.9572256 (0.5−1.5)	per day	Fitted
β_v	0.3212098 (0.2−1.25)	per day	fitted
v	0.6333842 (0.001−0.95)	per day	fitted
η	0.5746209 (3/20 - 7/10)	per day	fitted
ϕ	0.65 (0−1)	per day	assumed
τ_a	0.084 (0.05−0.1)	per day	[28, 34]
τ_1	0.06 (0.042−0.09)	per day	[28, 34]
τ_2	0.052 (0.042−0.09)	per day	[28, 34]
τ_v	0.08 (0.05−0.1)	per day	Levine and Earn (2022)
θ	1/7 (1/6 - 1/8)	per day	Levine and Earn (2022)
δ	0.015 (0.01−0.25)	per day	[13, 34]
κ_1	0.34 (0−1)	per day	assumed
κ_2	0.55 (0−0)	per day	assumed

mainland China for December 2022 to study the spike in symptomatic proportions. Ultimately, the model serves for validation, prediction, and examining various COVID-19 transmission scenarios, considering the variolation effect, to enhance policymaking in the design of effective control strategies.

3. Results

3.1. Assessment of various stages of infectiousness proportions of SARS-CoV-2 considering the effects of variolation

Figs. 3–6 illustrates a time series fraction of SARS-CoV-2 infection considering potential variolation effects at different initial circumstances based on the model's key parameters to examine the dynamics of SARS-CoV-2 infection considering usual and variolated transmission. Simulation results shown in Fig. 3(a–g) demonstrated that when the transmission rate fluctuates (by increasing or reducing the transmission rate parameter), the dynamics of the model vary. In particular, Fig. 3(b–d) shows that increasing or decreasing the transmission rate parameter by 10%, 25%, or 50% would have a less or negligible impact on the overall disease dynamics. However, decreasing the transmission rate parameter by more than 50% could significantly alter the disease dynamics, especially for highly transmissible diseases such as the omicron variant. This further shows that to reduce the spread of disease, particularly among an asymptomatic proportion of the population, it is imperative to identify strategies that would lower the transmission rate, thereby decreasing the spread of the disease in the community.

Similar results were obtained in Figs. 4–6 by altering the facemask-induced variolation transmission rate, probability of infection per contact, and the proportion of infection without clinical symptoms, respectively. Fig. 4(b–d) indicates that increasing or decreasing the transmission due to variolation could not significantly affect the overall transmission of the disease dynamics. This shows that the frequency of getting the disease through variolation does not reduce its severity. However, using a facemask can prevent the infection for a period of time. More data will be researched to investigate the actual scenario.

Furthermore, the results of Figs. 5 and 6 also show that altering the values of the probability of infection per contact and the proportion of infection without clinical symptoms could significantly affect the overall transmission dynamics of the disease. For instance, increasing the probability of infection per contact parameter could significantly reduce the spread of the disease through variolation. Similarly, decreasing the probability of infection per contact parameter dramatically reduces the spread of the disease from both asymptomatic and symptomatic infectious individuals. Fig. 6 shows a similar effect on the general dynamics, i.e., if the proportion of infection without clinical symptoms (η) changes, transmission due to variolation also alters. Increasing η by 10%, 25%, or 50% reduces the spread of the disease through variolation, just as it minimizes the spread of the disease from symptomatically infectious individuals. However, reducing the proportion of infection without clinical symptoms minimizes the disease's spread from asymptomatically infectious individuals and from variolated individuals. Whereas transmission from symptomatically infectious individuals remains unchanged (or slightly changed).

3.2. Assessing the effects of various incidence rates and reproduction number on the overall dynamics

In Fig. 7, we simulated various transmission rates for symptomatically (severe), asymptomatically, and variolated (mild) infectious individuals, respectively, to examine the general dynamics considering different transmission probabilities. The result shows the contribution of each incidence rate to the overall transmission of SAR-CoV-2. We observed that the contribution of FOI from asymptomatically infectious individuals is much higher for the rapid spread of the disease, followed by symptomatically mild infectious as well as variolated infectious individuals. FOI from symptomatically severe infectious individuals has the least contribution to the overall transmission dynamics of the disease. This aligns with several previous
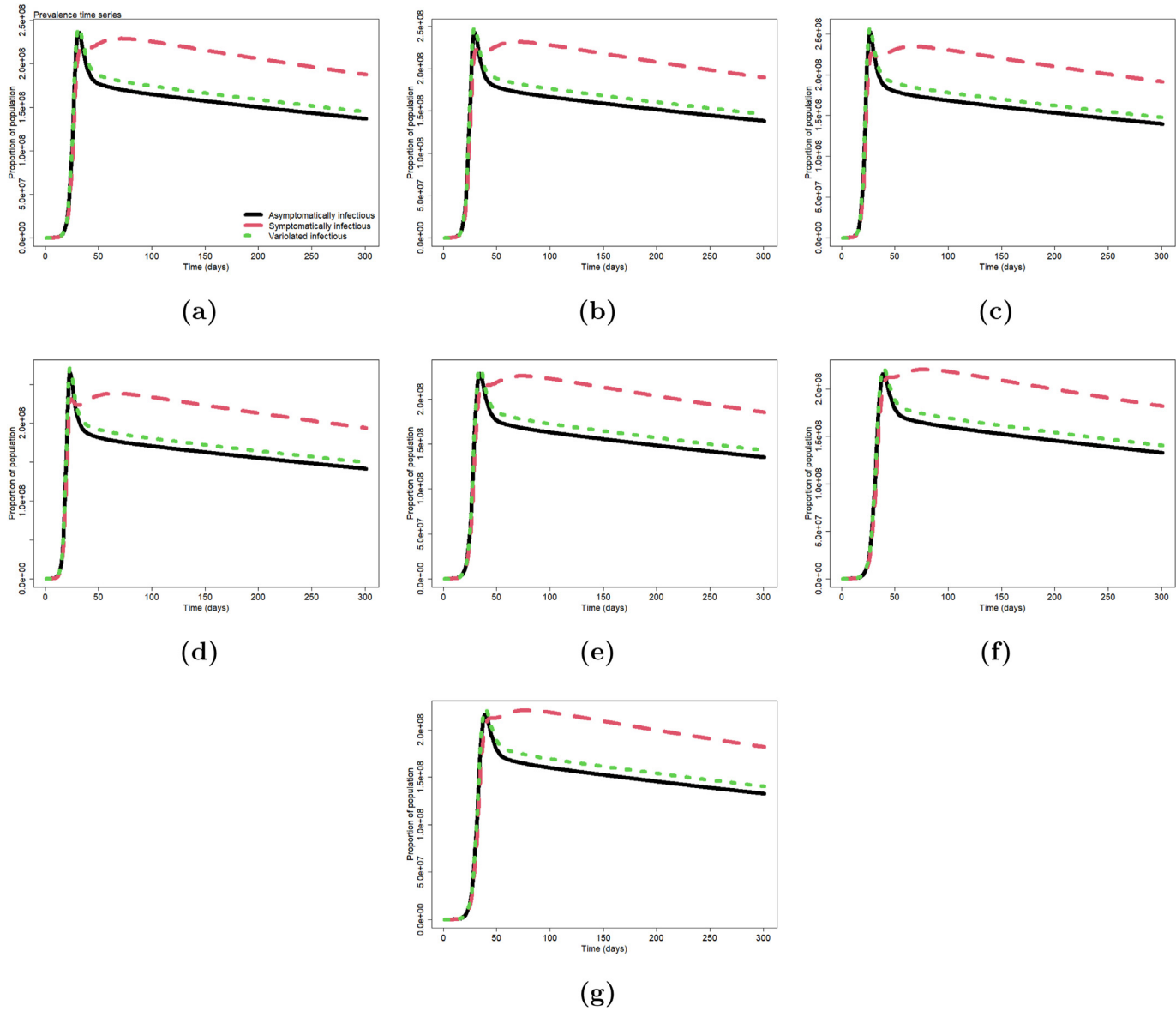
Fig. 3. Simulation of the model with potential variolation effects for different infection scales for asymptomatically, symptomatically, and variolated infectious individuals with varying transmission rates. Panel (a) shows the proportion of the population infected for the initial value of the transmission rate. Figures (b–d) show the proportion of the population infected with 10%, 25%, and 50% increase in the initial transmission rate, respectively. Figures (e–g) show the proportion of the population infected with 10%, 25%, and 50% decrease in the initial transmission rate, respectively.
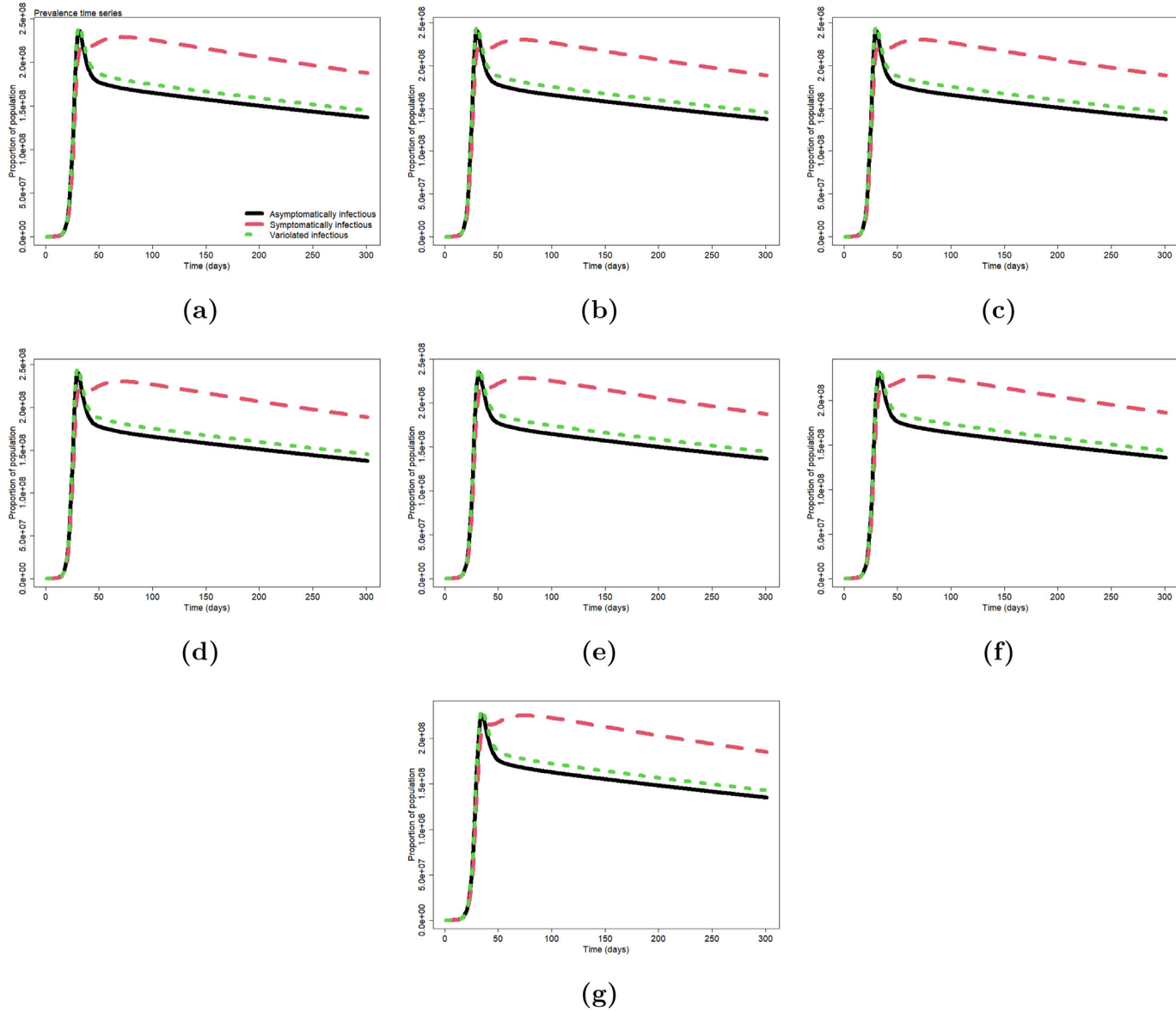
Fig. 4. Simulation of the model with potential variolation effects for different infection scales for asymptomatically, symptomatically, and variolated infectious individuals with varying variolated transmission rates. Panel (a) shows the proportion of the population infected for the initial value of the transmission rate due to variolation. Figures (b–d) show the proportion of the population infected with a 10%, 25%, and 50% increase in the initial transmission rate due to variolation, respectively. Figures (e–g) show the proportion of the population infected with 10%, 25%, and 50% decrease in the initial transmission rate due to variolation.
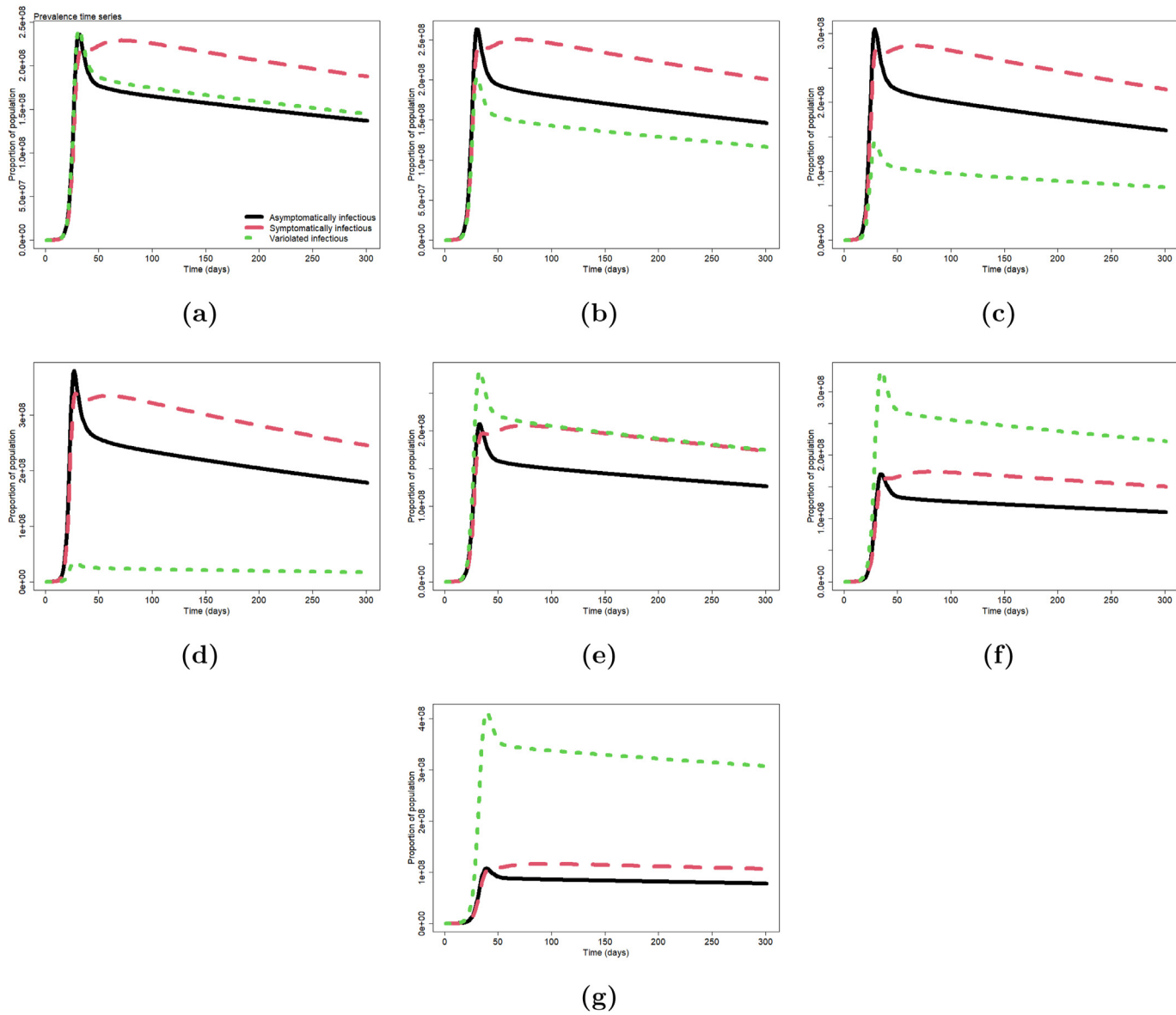
Fig. 5. Simulation of the model with potential variolation effects for different infection scales for each asymptomatically, symptomatically, and variolated infectious scenario with varying parameter values of the probability of infection per contact. Panel (a) shows the proportion of the population infected for the initial value of the probability of infection per contact. Panels (b–d) show the proportion of the population infected with a 10%, 25%, and 50% increase in the initial probability of infection per contact, respectively. Panels (e–g) show the proportion of the population infected with 10%, 25%, and 50% decrease in the initial probability of infection per contact, respectively.
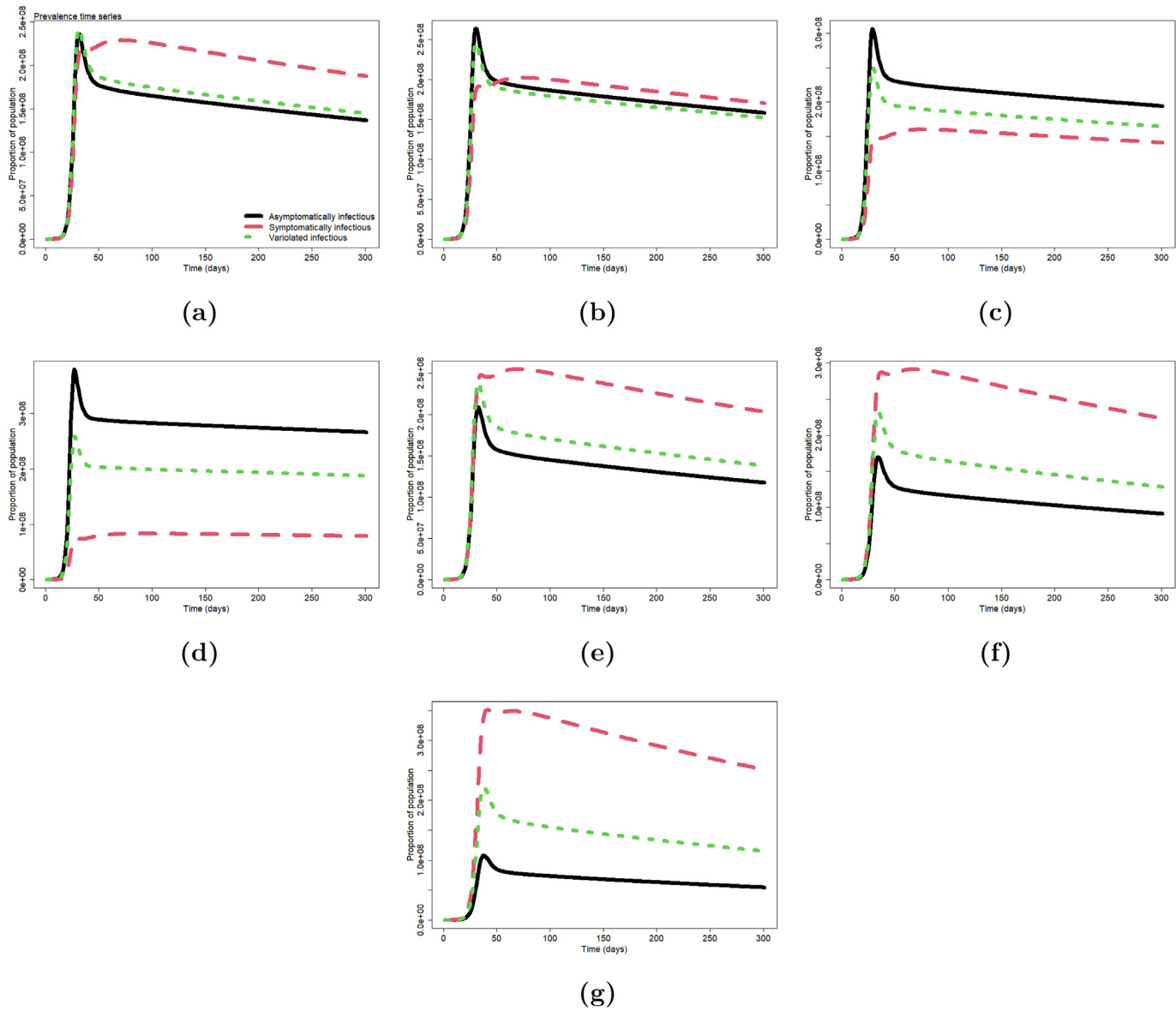
Fig. 6. Simulation of the model with potential variolation effects for different infection scales for each asymptomatically, symptomatically, and variolated infectious scenario with varying proportions of infection without clinical symptoms. Panel (a) shows the proportion of the population infected for the initial value of the proportion of infection without clinical symptoms. Figures (b–d) show the proportion of the population infected with 10%, 25%, and 50% increase in the initial proportion of infection without clinical symptoms, respectively. Panels (e–g) show the proportion of the population infected with 10%, 25%, and 50% decrease in the initial proportion of infection without clinical symptoms, respectively.
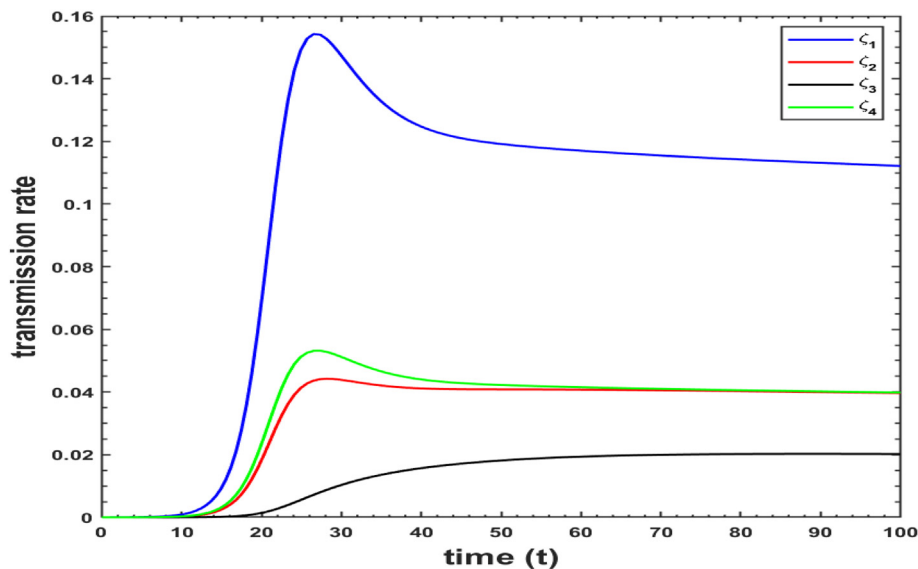
Fig. 7. Simulation results of the dynamics of the incidence function show the transmission behavior of SARS-CoV-2 obtained from the evolutionary equations in (2). The evolutionary dynamics of the transmission rates could vary based on the choice of parameter values given in Table 2. Each curve represents a different incidence function. That is, incidence functions ξ_1, ξ_2, ξ_3, and ξ_4 are represented by blue, red, black, and green colors.

works indicating that individuals with severe COVID-19 symptoms are less likely to spread the disease than asymptomatically infectious (or even mildly infected individuals) (Rasmussen & Popescu, 2021). This is because they are probably less energetic to move around or travel and, therefore, have a lower probability of spreading the disease. Also, people with severe symptoms are usually isolated from the community to prevent them from continuing to spread the disease.

Here, further simulations were conducted to evaluate the effect of $\mathcal{R}_0$ against some key parameters and how they affect the general transmission dynamics of the disease. Fig. 8 depicts the heat map (contour plots) of the basic reproductive number $\mathcal{R}_0$ as a function of different key epidemic parameters of the model (1). In particular, we evaluated $\mathcal{R}_0$ with respect to β, v, η, and β_v, which are crucial parameters that could help prevent and control COVID-19 spread in China and elsewhere. Table 2 gives all other parameter values. Fig. 8 (a) shows $\mathcal{R}_0$ increases with respect to the increase in the transmission rate (β), probability of infection per contact (v), proportion of infection without clinical symptoms (η), and transmission due to variolation (β_v). That is, increasing these parameters could significantly affect $\mathcal{R}_0$, thereby increasing the disease transmissibility. These parameters should be reduced significantly to reduce the transmission strength and prevent the disease spread.

4. Sensitivity analysis

Following prior studies (Gao et al., 2016; Musa et al., 2020), sensitivity analysis was performed using partial rank correlation coefficients (PRCCs) to identify the model's most influential parameters. In this case, the parameters $\mathcal{R}_0$ and infection attack rate (proportion of the population that gets infected with SARS-CoV-2 during the epidemic period). were chosen as reaction functions. Our sensitivity analysis results are depicted in Fig. 9. Five thousand random samples were drawn from uniform distributions using the parameter ranges listed in Table 2 for each model parameter. The model was simulated for each random parameter value to produce the desired biological quantities. The PRCCs were calculated between each parameter and the desired biological values.

The PRCC results presented in 9 indicate that the parameters β and β_v are top-ranked biological quantities to curtail the spread of SARS-CoV-2 in China, followed by the parameters τ_v and κ_1. Indicating that to curtail the transmission of SARS-CoV-2 in China effectively, there is a need to reduce the strength of β, β_v, and κ_1, whereas the parameter τ_v needs to be strengthened.

5. Discussion and conclusion

At a time when the rest of the world was easing COVID-19 policies due to fewer cases and less severe infections, China found itself in a challenging situation toward the end of 2022 due to a sudden increase in symptomatic proportions and hospitalizations in the number of COVID-19 cases, which caught public health attention. As a result, researchers and public health professionals look for potential reasons for this problem. However, the disease's transmissibility and severity have significantly declined in the current year. To understand the main drivers that caused this problem, we developed an epidemic model for SARS-CoV-2 to investigate the factors responsible for the increase in symptomatic proportions of SARS-CoV-2 in China. In particular, the overarching goals of this investigation were to improve understanding of COVID-19
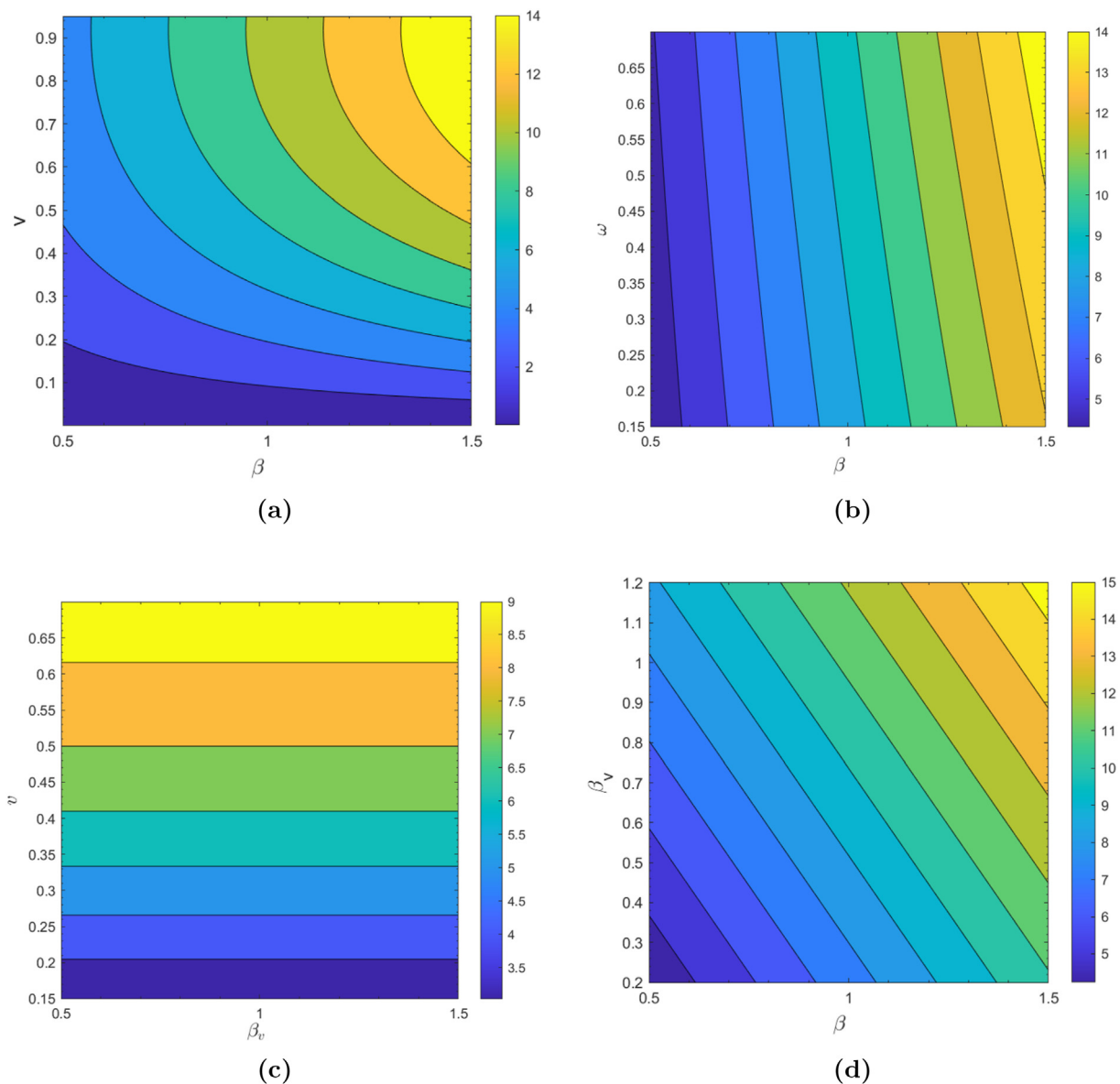
Fig. 8. Contour plots of the reproduction number of the model (1), as a function of (a) transmission rate due to usual infection (β) and Probability of infection per contact (v), (b) transmission rate due to usual infection (β) and ω, (c) transmission rate due to variolation (β_v) and Probability of infection per contact (v), and (d) transmission rate due to usual infection (β) and Transmission rate due to variolation (β_v), respectively. Parameter values used are given in Table 2.

dynamics by using a classical SEIR dynamic model, which incorporates both asymptomatic and symptomatic transmission as well as transmission due to variolation. This would plausibly provide more accurate estimations for crucial epidemiological metrics such as reproduction numbers, exponential growth rates, and serial intervals, which enhances control and pre-paredness measures for future epidemics or pandemics.

Our findings revealed feasible explanations for increased SARS-CoV-2 symptoms in China in December 2022. Among the possible causes are a spike in the number of cases during the winter and viral inhalation due to the large number of infected cases, which probably contributed to the illness's high transmissibility and severity. Our model also discussed the potential effects of facemask-induced variolation on decreasing or increasing SARS-CoV-2 transmissibility and severity. In particular, our model studies the roles of usual transmission and facemask-induced variolation transmission and quantifies the risks of infection for developing severe disease. Based on our findings, we hypothesized that an increase in viral inhalations (which enhances disease transmissibility and hospitalization) in the winter is a likely cause driving an increase in the symptomatic proportion of SARS-CoV-2 in China at the end of 2022. However, more epidemiological data is required to study this possibility further. According to (Howard et al., 2021), the expected and empirical estimates of the transmission bottleneck size
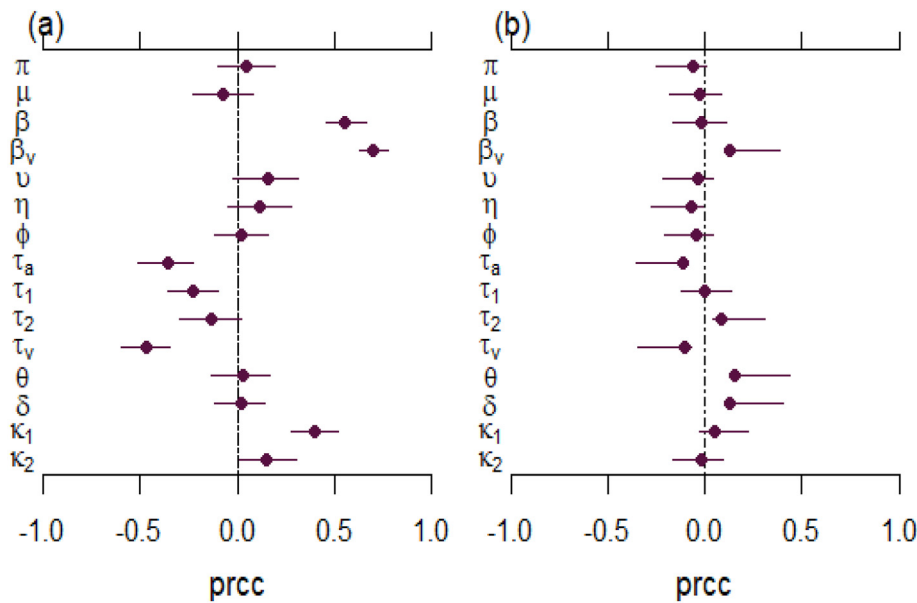
Fig. 9. The plot of the PRCCs of (a) $\mathcal{R}_0$ and (b) infection attack rate for the sensitivity analysis against the model parameters given in Table 2. The circle dots (in purple) are the estimated correlations, and the bars are the 95% CIs.

show that natural inoculum dosages are shallow, indicating that facial masking is anticipated to diminish transmission potential. Facemasks are unlikely to reduce the risk of contracting a severe illness (Koelle et al., 2022), but we suggest that further epidemiological investigation could help evaluate actual variolation effects.

Furthermore, our model was rigorously analyzed to assess crucial epidemiological qualities such as basic reproduction number, which is used in designing appropriate control measures. In Figs. 3–6, several simulations were also conducted to pinpoint the most critical parameters that affect the overall dynamics of the disease. To analyze the dynamics of the disease using different transmission probabilities, we simulated various transmission rates for symptomatically (severe), asymptomatically, and variolated (mild) infections in Fig. 7. To gain more insights into the disease dynamics, we simulated various incidence functions, one of the crucial epidemiological quantities that could also be used in designing appropriate intervention measures. In Fig. 7, we revealed the contribution of each force of infection to the overall transmission of the disease. The results of the contour plots in Fig. 8 also revealed the influence of some vital parameters on the overall transmission dynamics. The heat map (contour plots) of the basic reproductive number $\mathcal{R}_0$ as a function of two distinct essential parameters of the model (1) is shown in Fig. 8. We specifically assessed $\mathcal{R}_0$ in relation to β, υ, η, and β_v, respectively, which are essential parameters for preventing and controlling COVID-19 spread in China and elsewhere. In addition, PRCC results presented in Fig. 9 revealed the top-ranked biological quantities that need special emphasis to effectively curtail the disease spread in order of their preference. Those are: (i) β (ii) β_v (iii) τ_v, and (iv) κ_1. These are the most critical parameters from our analysis, and thus, they should be prioritized to control effectively and could help reduce the high symptomatic proportion of COVID-19 in China.

Infection due to facemask-induced variolation, generates milder symptoms compared to symptomatic infection since variolated infectious people are considered to have reduced symptoms due to their immune system reaction to the SARS-CoV-2. However, the precise proportion of symptoms might be influenced by several diseases and non-disease factors, such as the precise facemask utilized, the person's immune response, and the underlying health status. The proportion of SARS-CoV-2 variolated infections increases when infected individuals have milder symptoms since they can move around and transmit the disease faster compared to severely infected individuals. That is, people can get the immune system to respond without getting sick seriously by being exposed to a less dangerous version of the virus as opposed to severely symptomatic infection (when people are exposed to the full force of the virus, which results in a more significant proportion of symptomatic infections). This also indicates that variolation reduces the transmission rather than the severity of SARS-CoV-2.

It is important to emphasize that (intentional) variolation is not recommended for SARS-CoV-2 for various reasons, including the possibility of uncontrolled transmission, unpredictable immune responses, and the lack of safe and effective vaccinations. Vaccines have undergone extensive testing and are intended to protect against severe sickness and hospitalization while posing minimal risk. Vaccination campaigns are the principal technique health officials advocate for restricting the spread of SARS-CoV-2 and reducing the burden of symptomatic and severe cases. For the most up-to-date and evidence-based information on the prevention, control, and treatment of infectious diseases such as COVID-19, it is always critical to follow the advice of public health organizations and consult healthcare specialists. According to previous epidemiologic studies, wearing close facemasks only reduces SARS-CoV-2 transmission and acquisition rather than serving as a proxy for

vaccination or mitigating the severity of COVID-19 (Abaluck et al., 2022; Aydin et al., 2020; Gurbaxani et al., 2022; Howard et al., 2021; Koelle et al., 2022; Levine & Earn, 2022); nevertheless, more researches are needed to assess its possible variolation effects.

While our analysis provides useful insights into the COVID-19 epidemic dynamics in China, it is crucial to acknowledge some limitations and areas for further investigation. First, we investigate the causes of the increase in the symptomatic proportion of SARS-CoV-2 in China, although further data are needed to corroborate the findings and estimate vital epidemic metrics. Second, our models are simple, resulting in qualitative conclusions. As a result, findings are obtained analytically, allowing for qualitative inferences for crucial epidemic parameters such as reproduction numbers and generation intervals, supporting effective control interventions. Thirdly, regarding the notable formulation of the force of infection in the context of social distancing measures, where differential per-capita contact rates between individuals in different compartments may necessitate additional consideration, potentially including scenarios such as the proportional mixing assumption. While this is critical, it is worth noting that our approach to modeling the force of infection was based on established epidemiological principles and the available data. Although including differential contact rates could improve the model's realism, it could result in more complexity and uncertainty, which we intend to address in the future.

Ethics approval and consent to participate

Not applicable.

Availability of data and materials

All data utilized in this study were obtained from public sites.

CRediT authorship contribution statement

Salihu S. Musa: Conceptualization, Data curation, Formal analysis, Investigation, Methodology, Project administration, Resources, Software, Supervision, Validation, Visualization, Writing – original draft, Writing – review & editing. **Shi Zhao:** Formal analysis, Investigation, Methodology, Validation, Writing – original draft, Writing – review & editing. **Ismail Abdulrashid:** Investigation, Methodology, Writing – original draft, Writing – review & editing. **Sania Qureshi:** Formal analysis, Validation, Writing – original draft, Writing – review & editing. **Andress Colubri:** Investigation, Methodology, Supervision, Writing – review & editing. **Daihai He:** Conceptualization, Formal analysis, Funding acquisition, Investigation, Methodology, Project administration, Resources, Software, Supervision, Validation, Writing – original draft, Writing – review & editing.

Declaration of competing interest

DH is an associate editor of the journal but has no role in the review process. Another editorial board member handles the manuscript. All other authors declared no conflict of interest.

Acknowledgements

Appendix

A1. Model's basic properties

Since model (1) investigates the dynamics of COVID-19 transmission due to usual and variolation-related infection, all its state variables and parameters are assumed to be strictly positive. To examine the elementary qualitative features of model (1), we, first of all, consider the rate of change of the total human population ($N'(t)$), which is evaluated as

$$\frac{dN}{dt} = \pi - \mu N - \delta I_2 \leqslant \pi - \mu N. \tag{A1}$$

A1.1. Positivity of model solutions
For the model (1) to be biologically and epidemiologically reasonable, the state variables must be non-negative at all times $t > 0$. In other words, solutions of model (1) with positive initial data will always remain positive at $t > 0$.

Lemma A1.1.   *Let the initial data $\Theta(0) \geq 0$, where $\Theta(t) = (S, I_a, I_1, I_2, I_v, R, R_v)$. Then the solutions $\Upsilon(t)$ of model (1) are positive for all $t > 0$.*

Proof. Let $t^1 = sup\{t > 0 : \Theta(t) > 0 \in [0, t]\}$. Thus, $t^1 > 0$. Since π and $\theta(R + R_v)$ are positive, it follows from the first equation of the model (1) that

$$\frac{dS}{dt} \geq -(\zeta(t) + \mu)S. \tag{A2}$$

Following the comparison theorem in conjunction with the separation of variables method (Hussaini et al., 2017; Roop-O, Chinviriyasit, & Chinviriyasit, 2015), we have

$$S(t^1) \geq S_n(0)exp\left[- \left(\int_0^{t_1} \zeta(u)du + (\mu)t_1 \right) \right] > 0. \tag{A3}$$

Hence, $S(t) > 0$. Similarly, it can be shown that the remaining components of $\Theta(t)$, i.e., $I_a, I_1, I_2, I_v, R, R_v$ are all positive for all $t > 0$. Hence, $\Theta(t) > 0$ for all $t > 0$. □

A1.2. Invariant region

Following previous studies (Hussaini et al., 2017; Roop-O et al., 2015), we consider the following biologically feasible region:

$$\Omega = \left\{ (S, I_a, I_1, I_2, I_v, R, R_v) \in \mathbb{R}_+^7 : N \leqslant \frac{\pi}{\mu} \right\}.$$

Since N is positive, to ensure that any solutions of the system that start in the region Ω remain in Ω for all non-negative time t, it is sufficient to look at solutions that are limited to Ω, which is positively-invariant. Therefore, the results for a normal existence, uniqueness, and continuity will be satisfied for model (1) per earlier works (Hussaini et al., 2017; Roop-O et al., 2015).

A2. Disease-free equilibrium and Ro computation

Disease-free equilibrium (DFE) of model (1), denoted by Γ^0, is obtained by setting all the equations of the right-hand side of model (1) to zero, that is $\frac{dS}{dt} = \frac{dI_a}{dt} = \frac{dI_1}{dt} = \frac{dI_2}{dt} = \frac{dI_2}{dt} = \frac{dI_v}{dt} = \frac{dR}{dt} = \frac{dR_v}{dt} = 0$. This yields $S^0 = \frac{\pi}{\mu}, I_a^0 = I_1^0 = I_2^0 = I_v^0 = R^0 = R_v^0 = 0$. Thus, the DFE for model (1) is given by

$$\Gamma^0 = \{S^0, I_a^0, I^1, I_2^0, I_v^0, R^0, R_v^0\} = \left\{ \frac{\pi}{\mu}, 0, 0, 0, 0, 0, 0 \right\}. \tag{A4}$$

To compute $\mathcal{R}_0$, we employed the approach proposed in (Diekmann et al., 1990; Van den Driessche, 2017; Van den Driessche & Watmough, 2002). First, we obtained the linear stability for the DFE by using the technique of the NGM for the proposed model (1). The matrices F and V represent the new infection terms and other transfer terms, respectively, and are given by

$$F = \begin{bmatrix} \eta\nu\beta & \eta\nu\beta k_1 & \eta\nu\beta k_2 & \eta\nu\beta_v \\ (1-\eta)\nu\beta & (1-\eta)\nu\beta k_1 & (1-\eta)\nu\beta k_2 & (1-\eta)\nu\beta_v \\ 0 & 0 & 0 & 0 \\ (1-\nu)\beta & (1-\nu)\beta k_1 & (1-\nu)\beta k_2 & (1-\nu)\beta_v \end{bmatrix}, \quad \text{and} \tag{A5}$$

$$V = \begin{bmatrix} p_1 & 0 & 0 & 0 \\ 0 & p_2 & 0 & 0 \\ 0 & -(1-\varphi)\tau_1 & p_3 & 0 \\ 0 & 0 & 0 & p_4 \end{bmatrix}. \tag{A6}$$

Hence, by direct calculation from the above equations (A5) and (A6), $\mathcal{R}_0$ is obtained as follows $\mathcal{R}_0 = \rho(FV^{-1}) = \mathcal{R}_a + \mathcal{R}_1 + \mathcal{R}_2 + \mathcal{R}_v$,

where $p_1 = \tau_a + \mu$, $p_2 = \tau_1 + \mu$, $p_3 = \tau_2 + \delta + \mu$, $p_4 = \tau_v + \mu$, and ρ represents the spectral radius of the next-generation matrices.

The result of Theorem A2.1 follows from Theorem 2 of (Van den Driessche & Watmough, 2002), and reference to the local stability of the DFE of model (1), the result of Theorem 3.1 below follows.

Theorem A2.1.   *The disease-free equilibrium of model (1) is locally-asymptotically stable whenever $\mathcal{R}_0 \leq 1$.*

The epidemiological significance of the above theorem indicates that a paltry SARS-CoV-2 infection would not potentially generate a large outbreak when $\mathcal{R}_0 < 1$. To prevent large attacks of SARS-CoV-2, the requirement for making $\mathcal{R}_0$ less than 1 is suitable but unneeded. Thus, when $\mathcal{R}_0$ decreases to a value less than 1, the disease eventually fades, while the disease persists when $\mathcal{R}_0$ increases to more than 1. Consequently, more sophisticated intervention measures are required to mitigate the disease effectively (Van den Driessche, 2017). For details of theoretical analysis, see Appendices A1-A3.

A3. Endemic equilibrium and its stability

The endemic equilibria (EE) of model (1) are the steady states where the disease may persist in the population, i.e., when at least one of the infected compartments of model (1) is non-empty. Thus, by setting the vector field of system (1) to zero, we get endemic equilibrium states following some algebraic computations. Thus, the endemic equilibrium points are represented by

$$\Gamma^* = \{S^*, I_a^*, I_1^*, I_2^*, I_v^*, R^*, R_v^*\}. \tag{A7}$$

In terms of $\zeta*$, the EE points are given by the following equations

$$
\begin{aligned}
S^* &= \frac{p_2 p_3 I_2}{(1-\eta)v\zeta(1-\varphi)\tau_1}, \\
I_a^* &= \frac{\eta p_2 p_3 I_2}{p_1(1-\eta)(1-\varphi)\tau_1}, \\
I_1^* &= \frac{p_3 I_2}{(1-\varphi)\tau_1}, \\
I_v^* &= \frac{(1-v)p_2 p_3 I_2}{p_4(1-\eta)v(1-\varphi)\tau_1}, \\
R^* &= \frac{(\tau_a \eta p_2 p_3 + \varphi p_1 p_3(1-\eta)\tau_1 + \tau_2 p_1(1-\eta)(1-\varphi)\tau_1)I_2}{p_1 p_5(1-\eta)(1-\varphi)\tau_1}, \quad \text{and} \\
R_v^* &= \frac{\tau_v(1-v)p_2 p_3 I_2}{p_4 p_5(1-\eta)v(1-\varphi)\tau_1}.
\end{aligned}
\tag{A8}
$$

The presence of EE in the model suggests that at least one of the model's infected classes is not empty, implying that the disease spreads and endures in a community.

The model's solutions in the interior of the feasible region converge to the unique EE, given by $\Gamma*$, whenever $\mathcal{R}_0 > 1$. Thus, at $\Gamma*$, the disease will spread and persist in a community. To prove the global stability of the EE, we can employ a Lyapunov function technique (LaSalle, 1976), which is attainable by constructing the Lyapunov function from the model. This technique has been used largely in previous studies; see, for instance, (Hussaini et al., 2017; LaSalle, 1976; Roop-O et al., 2015; Yang, Wang, Gao, & Wang, 2017), and the references therein. In the current mode, we skip the GAS proof of the EE since our model is an extension of the model in (Korobeinikov, 2009; Levine & Earn, 2022), and a similar proof has been obtained. The Theorem asserts that the EE, $\Gamma*$, is globally-asymptotically stable (GAS) in the region Ω whenever $\mathcal{R}_0 > 1$.

A4. Epidemic data and model parameters

We downloaded "COVID-19" situation reports from the World Health Organization (WHO) disease surveillance systems (World Health Organization, 2023), which include the observed number of infected cases and the number of mortalities in China. We used the data covering December 1−31, 2022, for model validation. We chose this period since it is consistent with the aim of the study. That is, to reveal the potential factors for the increase in the symptomatic proportion of SARS-CoV-2 in China in December 2022.

From the fitting reults in Fig. 2, we estimated the following crucial biological parameters that are used for further simulations: $\beta = 0.9572256$, $\beta_v = 0.3212098$, $v = 0.6333842$ and $\eta = 0.5746209$. The initial conditions for the model's state variables used in the fitting processes are $S(0) = 1 \times 10^9$; $I_a(0) = 13429$; $I_1(0) = 6500$; $I_2(0) = 3000$; $I_v(0) = 1000$; $R(0) = 650$; and $R_v(0) = 100$. For other model parameters, see Table 2. Furthermore, based on previous studies, $\mathcal{R}_0$ and other key epidemic parameters could be estimated; see, for instance, (Jalali et al., 2022; Levine & Earn, 2022; Li et al., 2020; Worldometer, 2023) and the references therein. Therefore, the reasonable fitting results imply that the model could be employed to forecast and analyze SARS-CoV-2 dynamics in a community.

References

Abaluck, J., Kwong, L. H., Styczynski, A., Haque, A., Kabir, M. A., Bates-Jefferys, E., et al. (2022). Impact of community masking on COVID-19: A cluster-randomized trial in Bangladesh. *Science, 375*(6577), Article eabi9069.

Anderson, R. M., & May, R. M. (1991). *Infectious diseases of humans: Dynamics and control.* Oxford University Press.

Aydin, O., Emon, B., Cheng, S., Hong, L., Chamorro, L. P., & Saif, M. T. (2020). Performance of fabrics for home-made masks against the spread of COVID-19 through droplets: A quantitative mechanistic study. *Extreme Mechanics Letters, 40,* Article 100924.

Bielecki, M., Züst, R., Siegrist, D., Meyerhofer, D., Crameri, G. A., Stanga, Z., et al. (2021). Social distancing alters the clinical course of COVID-19 in young adults: A comparative cohort study. *Clinical Infectious Diseases, 72*(4), 598–603.

Biology Online. Inoculum https://www.biologyonline.com/dictionary/inoculum. Accessed on March 13, 2023.

Brosseau, L. M., Roy, C. J., & Osterholm, M. T. (2020). Facial masking for Covid-19. *New England Journal of Medicine, 383*(21), 2092–2093.

Cai, M., Bowe, B., Xie, Y., & Al-Aly, Z. (2021). Temporal trends of COVID-19 mortality and hospitalisation rates: An observational cohort study from the US department of veterans affairs. *BMJ Open, 11*(8), Article e047369.

China CDC Weekly https://weekly.chinacdc.cn/. December 30, 2023..

Del Rio, C., & Malani, P. N. (2022). COVID-19 in 2022—the beginning of the end or the end of the beginning? *JAMA, 327*(24), 2389–2390.

Diekmann, O., Heesterbeek, J. A., & Metz, J. A. (1990). On the definition and the computation of the basic reproduction ratio Ro in models for infectious diseases in heterogeneous populations. *Journal of Mathematical Biology, 28*(4), 365–382.

Eikenberry, S. E., Mancuso, M., Iboi, E., Phan, T., Eikenberry, K., Kuang, Y., et al. (2020). To mask or not to mask: Modeling the potential for face mask use by the general public to curtail the COVID-19 pandemic. *Infectious Disease Modelling, 5,* 293–308.

Ferguson, N., Laydon, D., Nedjati Gilani, G., Imai, N., Ainslie, K., Baguelin, M., et al. (2020). *Report 9: Impact of non-pharmaceutical interventions (NPIs) to reduce COVID-19 mortality and healthcare demand.* London: Imperial College. https://spiral.imperial.ac.uk/handle/10044/1/77482.

Gandhi, M., Beyrer, C., & Goosby, E. (2020c). Masks do more than protect others during COVID-19: Reducing the inoculum of SARS-CoV-2 to protect the wearer. *Journal of General Internal Medicine, 35*(10), 3063–3066.

Gandhi, M., & Rutherford, G. W. (2020a). Facial masking for Covid-19—potential for "variolation" as we await a vaccine. *New England Journal of Medicine, 383*(18), Article e101.

Gandhi, M., & Rutherford, G. W. (2020b). Facial masking for Covid-19. Reply. *New England Journal of Medicine, 383,* 2093–2094.

Gao, D., Lou, Y., He, D., Porco, T. C., Kuang, Y., Chowell, G., et al. (2016). Prevention and control of zika as a mosquito-borne and sexually transmitted disease: A mathematical modeling analysis. *Scientific Reports, 6*(1), Article 28070.

Guallar, M. P., Meiriño, R., Donat-Vargas, C., Corral, O., Jouvé, N., & Soriano, V. (2020). Inoculum at the time of SARS-CoV-2 exposure and risk of disease severity. *International Journal of Infectious Diseases, 97,* 290–292.

Gurbaxani, B. M., Hill, A. N., Paul, P., Prasad, P. V., & Slayton, R. B. (2022). Evaluation of different types of face masks to limit the spread of SARS-CoV-2: A modeling study. *Scientific Reports, 12*(1), 8630.

Howard, J., Huang, A., Li, Z., Tufekci, Z., Zdimal, V., Van Der Westhuizen, H. M., et al. (2021). An evidence review of face masks against COVID-19. *Proceedings of the National Academy of Sciences, 118*(4), Article e2014564118.

Hussaini, N., Okuneye, K., & Gumel, A. B. (2017). Mathematical analysis of a model for zoonotic visceral leishmaniasis. *Infectious Disease Modelling, 2*(4), 455–474.

Jalali, N., Brustad, H. K., Frigessi, A., MacDonald, E. A., Meijerink, H., Feruglio, S. L., et al. (2022). Increased household transmission and immune escape of the SARS-CoV-2 Omicron compared to Delta variants. *Nature Communications, 13*(1), 5706.

Jewell, N. P., & Lewnard, J. A. (2022). On the use of the reproduction number for SARS-CoV-2: Estimation, misinterpretations and relationships with other ecological measures. *Journal of the Royal Statistical Society - Series A: Statistics in Society, 185*(Supplement-1), S16–S27.

Kermack, W. O., & McKendrick, A. G. (1927). A contribution to the mathematical theory of epidemics. *Proceedings of the Royal Society of London. Series A., 115*(772), 700–721.

Koelle K, Lin J, Zhu H, Antia R, Lowen A, Weissman D. (2022). Masks Do No More Than Prevent Transmission: Theory and Data Undermine the Variolation Hypothesis. *medRxiv.* 2022-06 https://doi.org/10.1101/2022.06.28.22277028..

Korobeinikov, A. (2009). Global properties of SIR and SEIR epidemic models with multiple parallel infectious stages. *Bulletin of Mathematical Biology, 71,* 75–83.

LaSalle, J. P. (1976). *The stability of dynamical systems. Regional conference series in applied mathematics.* Philadelphia: Soceity for Industrial and Applied Mathematics.

Levine, Z., & Earn, D. J. (2022). Face masking and COVID-19: Potential effects of variolation on transmission dynamics. *Journal of The Royal Society Interface, 19*(190), Article 20210781.

Li, R., Pei, S., Chen, B., Song, Y., Zhang, T., Yang, W., et al. (2020). Substantial undocumented infection facilitates the rapid dissemination of novel coronavirus (SARS-CoV-2). *Science, 368*(6490), 489–493.

Lin, Q., Zhao, S., Gao, D., Lou, Y., Yang, S., Musa, S. S., et al. (2020). A conceptual model for the coronavirus disease 2019 (COVID-19) outbreak in Wuhan, China with individual reaction and governmental action. *International Journal of Infectious Diseases, 93,* 211–216.

Louie, J. K., Stoltey, J. E., Scott, H. M., Trammell, S., Ememu, E., Samuel, M. C., et al. (2022). Comparison of symptomatic and asymptomatic infections due to severe acute respiratory coronavirus virus 2 (SARS-CoV-2) in San Francisco long-term care facilities. *Infection Control & Hospital Epidemiology, 43*(1), 123–124.

Musa, S. S., Zhao, S., Gao, D., Lin, Q., Chowell, G., & He, D. (2020). Mechanistic modelling of the large-scale Lassa fever epidemics in Nigeria from 2016 to 2019. *Journal of Theoretical Biology, 493,* Article 110209.

Ngonghala, C. N., Iboi, E., Eikenberry, S., Scotch, M., MacIntyre, C. R., Bonds, M. H., et al. (2020). Mathematical assessment of the impact of non-pharmaceutical interventions on curtailing the 2019 novel Coronavirus. *Mathematical Biosciences, 325,* Article 108364.

Nogrady, B. (2020). What the data say about asymptomatic COVID infections. *Nature, 587*(7835), 534–535.

Rasmussen, A. L., Escandón, K., & Popescu, S. V. (2020). Facial masking for ovid-19. *New England Journal of Medicine, 383*(21), 2092.

Rasmussen, A. L., & Popescu, S. V. (2021). SARS-CoV-2 transmission without symptoms. *Science, 371*(6535), 1206–1207.

Roop-O, P., Chinviriyasit, W., & Chinviriyasit, S. (2015). The effect of incidence function in backward bifurcation for malaria model with temporary immunity. *Mathematical Biosciences, 265,* 47–64.

Statista. Birth rate in China from 2000 to 2022 https://www.statista.com/statistics/251045/birth-rate-in-china/#::text=In%202022%2C%20the%20number%20of,a%20negative%20population%20growth%20rate.. Accessed March 21, 2023..

Tang, B., Bragazzi, N. L., Li, Q., Tang, S., Xiao, Y., & Wu, J. (2020). An updated estimation of the risk of transmission of the novel coronavirus (2019-nCov). *Infectious disease modelling, 5,* 248–255.

The World Bank. Life expectancy at birth, total (years) - China https://data.worldbank.org/indicator/SP.DYN.LE00.IN?locations=CN. Accessed March 21, 2023..

Trunfio, M., Longo, B. M., Alladio, F., Venuti, F., Cerutti, F., Ghisetti, V., et al. (2021). On the SARS-CoV-2 "variolation hypothesis": No association between viral load of index cases and COVID-19 severity of secondary cases. *Frontiers in Microbiology, 12,* Article 646679.

Van Damme, W., Dahake, R., Van de Pas, R., Vanham, G., & Assefa, Y. (2021). COVID-19: Does the infectious inoculum dose-response relationship contribute to understanding heterogeneity in disease severity and transmission dynamics? *Medical Hypotheses, 146,* Article 110431.

Van den Driessche, P. (2017). Reproduction numbers of infectious disease models. *Infectious Disease Modelling, 2*(3), 288–303.

Van den Driessche, P., & Watmough, J. (2002). Reproduction numbers and sub-threshold endemic equilibria for compartmental models of disease transmission. *Mathematical Biosciences, 180*(1–2), 29–48.

World Health Organization. WHO Coronavirus (COVID-19) Dashboard. https://covid19.who.int/data. Accessed March 21, 2023.

Worldometer. China Population. https://www.worldometers.info/world-population/china-population/. Accessed March 21, 2023.

Yang, C., Wang, X., Gao, D., & Wang, J. (2017). Impact of awareness programs on cholera dynamics: Two modeling approaches. *Bulletin of Mathematical Biology, 79,* 2109–2131.